Journal of Controlled Release 353 (2023) 823–831

Contents lists available at ScienceDirect

Journal of Controlled Release

journal homepage: www.elsevier.com/locate/jconrel

Development of poly(lactide-*co*-glycolide) microparticles for sustained delivery of meloxicam

Yihua Pei [a], Jianping Wang [a], Nisar Ul Khaliq [a], Fanfei Meng [a], Kaoutar A. Oucherif [b], Jie Xue [c], Sarena D. Horava [b], Amy L. Cox [c], Coralie A. Richard [c], Monica R. Swinney [b,1], Kinam Park [a,d], Yoon Yeo [a,d,*]

[a] Department of Industrial and Physical Pharmacy, Purdue University, 575 Stadium Mall Drive, West Lafayette, IN 47907, USA
[b] Eli Lilly and Company, 450 Kendall Street, Cambridge, MA 02142, USA
[c] Eli Lilly and Company, 893 Delaware Street, Indianapolis, IN 46225, USA
[d] Weldon School of Biomedical Engineering, Purdue University, West Lafayette, IN 47907, USA

ARTICLE INFO

Keywords:
Meloxicam
PLGA microparticles
Sustained drug delivery
Release kinetics control
In vitro-in vivo correlation

ABSTRACT

Poly(lactide-*co*-glycolide) (PLGA) polymers have been widely used for drug delivery due to their biodegradability and biocompatibility. One of the objectives of encapsulating a drug in PLGA microparticles (MPs) is to achieve an extended supply of the drug through sustained release, which can range from weeks to months. Focusing on the applications needing a relatively short-term delivery, we investigated formulation strategies to achieve a drug release from PLGA MPs for two weeks, using meloxicam as a model compound. PLGA MPs produced by the traditional oil/water (O/W) single emulsion method showed only an initial burst release with minimal increase in later-phase drug release. Alternatively, encapsulating meloxicam as solid helped reduce the initial burst release. The inclusion of magnesium hydroxide [$Mg(OH)_2$] enhanced later-phase drug release by neutralizing the developing acidity that limited the drug dissolution. The variation of solid meloxicam and $Mg(OH)_2$ quantities allowed for flexible control of meloxicam release, yielding MPs with distinct *in vitro* release kinetics. When subcutaneously injected into rats, the MPs with relatively slow *in vitro* drug release kinetics showed *in vivo* drug absorption profiles consistent with *in vitro* trend. However, the MPs that rapidly released meloxicam showed an attenuated *in vivo* absorption, suggesting premature precipitation of fast-released meloxicam. In summary, this study demonstrated the feasibility of controlling drug release from the PLGA MPs over weeks based on the physical state of the encapsulated drug and the inclusion of $Mg(OH)_2$ to neutralize the microenvironmental pH of the MPs.

1. Introduction

Poly(lactide-*co*-glycolide), also known as poly(lactic-*co*-glycolic acid) (PLGA), have been widely used for sustained drug delivery due to the biodegradability, safety, and commercial availability of the polymers. PLGA has been developed into microparticles (MP), solid implants, and *in situ* forming depots. Fourteen PLGA MP products have been approved by the United States Food and Drug Administration (US FDA) for various indications, such as cancer, diabetes, and inflammatory diseases [1,2]. The goal of most MP products is to maintain an effective plasma drug concentration for the desired period by providing an extended supply of a drug. Such MPs help reduce the frequency of administration and adverse effects related to drug level fluctuation, thus improving the effectiveness of therapy and the experience of patients.

The development of PLGA MP products requires tunable control of drug release kinetics according to the application. For example, PLGA MPs may be used for sustained delivery of non-steroidal anti-inflammatory drugs (NSAIDs) to achieve opioid-sparing analgesia in post-operative care [3]. A drug release duration of <2-week is preferable for this application [4], since an extended use of NSAIDs can interfere with wound healing [5]. A common approach to control the drug release kinetics is to vary the type of PLGA (molecular weight, lactic acid to glycolic acid ratio, and end group), solvents, polymer concentration, drug/polymer ratio, or conditions in the microencapsulation process

* Corresponding author at: Department of Industrial and Physical Pharmacy, Purdue University, 575 Stadium Mall Drive, West Lafayette, IN 47907, USA.
E-mail address: yyeo@purdue.edu (Y. Yeo).
[1] Current affiliation: LiquiGlide Inc., Cambridge, USA.

https://doi.org/10.1016/j.jconrel.2022.12.019
Received 7 September 2022; Received in revised form 7 December 2022; Accepted 8 December 2022

(emulsification speed, solvent removal, and annealing) [6–8]. However, it can be challenging to achieve a drug release control over 1–2 weeks, a time frame shorter than the degradation half-life of most commercially available PLGA. Moreover, drugs with ever-changing properties (*e.g.*, solubility or stability) in the MP microenvironment bring additional challenges to the release kinetics control [9–12], calling for formulation strategies to maintain them in an active and releasable form.

In this study, we developed PLGA MPs for sustained delivery of meloxicam, an NSAID selectively inhibiting cyclooxygenase-2. Meloxicam is indicated for treating rheumatoid arthritis and osteoarthritis and is available primarily as an oral formulation [13]. Given the elimination half-life of 20 h [14] and gastrointestinal side effects common to NSAIDs [15], it is desirable to develop a sustained release formulation that can deliver meloxicam over 1–2 weeks for its long-anticipated use in opioid-sparing postoperative analgesia [16]. However, meloxicam has a low water solubility, which decreases further in acidic pH (266 μg/mL at pH 7; < 3 μg/mL at < pH 5 [17]). This makes it difficult to control the drug release from MPs made of PLGA, which generates increasingly acidic pH upon degradation [18,19].

Given the relatively short target duration of drug release and the unique solubility profile of meloxicam, we varied the type of PLGA and the physical state of the loaded meloxicam (*i.e.*, dissolved or dispersed as solid) or introduced magnesium hydroxide [$Mg(OH)_2$] as a release modifier. The Design of Experiment (DoE) screening suggests that the status and content of the loaded drug as well as the use of $Mg(OH)_2$ have distinct effects on the initial burst release and later-phase release phase. We evaluated pharmacokinetics (PK) of meloxicam-loaded MPs with three different *in vitro* release kinetics, built an *in vitro-in vivo* correlation (IVIVC), and discussed the potential effect of drug release rate on *in vivo* performance.

2. Materials and methods

2.1. Materials

Poly(D,L-lactide-*co*-glycolide) polymers with a lactide:glycolide (L:G) ratio of 50:50 and ester-capped terminus (Resomers 502, 503, 504, and 505) were purchased from Sigma-Aldrich (St. Louis, MO, USA). Meloxicam and polyethylene glycol (molecular weight [MW] = 35,000 Da [Da]) were purchased from Sigma-Aldrich. Magnesium hydroxide and zinc carbonate basic were purchased from Alfa Aesar (Haverhill, MA, USA). Magnesium phosphate tribasic hydrate ($[Mg_3(PO_4)_2]\cdot xH_2O$) was purchased from ACROS Organics (Geel, Belgium). The magnesium standard for Atomic Absorption Spectroscopy (AAS) was purchased from Sigma-Aldrich. Poly(vinyl alcohol) (PVA, MW = 6000 Da) was purchased from Polysciences Inc. (Warrington, PA, USA).

2.2. Development of meloxicam-loaded PLGA microparticles

2.2.1. Variation of PLGA molecular weight (A, B, C; Table 1)

Meloxicam-loaded PLGA microparticles (MPs) were initially produced by the oil-in-water (O/W) single emulsion solvent evaporation method with PLGA of different molecular weights (Table 1). Briefly, 10 mg of meloxicam and 50 mg of PLGA (L:G = 50:50, ester end group) were dissolved in a 4:1 *v*/v mixture of dichloromethane (DCM) and dimethyl sulfoxide (DMSO). This meloxicam-PLGA solution was emulsified in 10 mL of 1% PVA solution with a Silverson® homogenizer (East Longmeadow, MA, USA) at 1500 rpm for 1 min. The emulsion was added to 25 mL of deionized (DI) water and stirred for 2.5 h at room temperature, followed by rotary evaporation under reduced pressure (500–600 mbar for 5 min and 20–30 mbar for 10 min) at room temperature. The MPs were collected by centrifugation at 2095 RCF for 5 min, washed with DI water twice, lyophilized with a Labconco freeze-dryer (Kansas City, MO, USA), and stored at −20 °C.

2.2.2. Modification of MP formulation (D, M4-M12, P4-P8; Table 2)

Three modifications were made to the MP formulation to suppress the initial burst release and enhance drug release later. The first modification involved increasing the meloxicam to PLGA weight ratio from 1:5 to 2:5. The second was to encapsulate meloxicam as a solid in the MPs. DMSO was omitted from the organic (O) phase, and meloxicam was suspended in DCM and emulsified in PVA solution (*i.e.*, solid-in-oil-in-water (S/O/W) emulsion method). The third modification involved including $Mg(OH)_2$ to neutralize the potential acidity of the MP matrices. With the three modifications combined, 40 mg of meloxicam and varying amounts of $Mg(OH)_2$ (or $Mg_3(PO_4)_2$ for comparison) were dispersed as solid in 0.5 mL of DCM containing 100 mg of PLGA (L:G = 50:50; ester-end; 7–17 kDa) to form a solid-in-oil (S/O) suspension. The S/O suspension was sonicated with a SONICS Vibra-Cell ultrasonic liquid processor (Newtown, CT, USA) run at 20% amplitude with a 1-s-on and 1-s-off duty cycle for 20 s to reduce the size of suspended solid particles (meloxicam and bases/salts). The volume median diameters of meloxicam, $Mg(OH)_2$, and $Mg_3(PO_4)_2$ sonicated in DCM in the same manner were 8.6 ± 0.62 μm, 3.4 ± 0.14 μm, and 20.9 ± 2.2 μm, respectively (Supporting Fig. 1). The suspension was then added to 10 mL of 1% PVA solution and emulsified at 1500 rpm for 1 min. The resultant S/O/W emulsion was mixed with an additional 25 mL of water, and the DCM was immediately removed by rotary evaporation under reduced pressure (500–600 mbar for 10 min and 20–30 mbar for 10 min) at room temperature. The MPs were collected, washed, lyophilized, and stored in the same manner as Section 2.2.1.

2.2.3. Design-of-Experiment (DoE; Table 3)

To optimize the drug release kinetics, DoE was performed following the response surface model, with $Mg(OH)_2$ content and meloxicam feed being two variables. The extent of drug release by the first 8 h and later-stage (8 h–7 days) drug release rate, expressed as k in $Q = kt^{0.5}$ (Higuchi model, Q: cumulative drug release (%); t: time (day); k: release constant), were used as responses. A randomized central composite design was employed, with four full factorial design points, four axial points, and eight central points (Table 3). The second order polynomial equation was used for the prediction of the effect of formulation variables on the responses. Each response (Y) was presented by a quadratic equation of the response surface. The modeling and response plot were performed using R 3.6.0 software with a backward, stepwise linear regression analysis, and significant terms ($P < 0.05$) were selected for final equations.

$$Y_i = b_0 + b_1X_1 + b_2X_2 + b_{12}X_1X_2 + b_{11}X_1^2 + b_{22}X_2^2.$$

Table 1
Formulation of meloxicam-loaded PLGA MPs produced by O/W emulsion method.

	PLGA	MW (kDa)	Meloxicam (mg)	PLGA (mg)	DCM (mL)	DMSO (mL)
A	Resomer 502	7–17	10	50	0.5	0.125
B	Resomer 503	24–38	10	50	0.5	0.125
C	Resomer 504	38–54	10	50	0.5	0.125

Table 2
Formulation of modified meloxicam-loaded PLGA MPs.

MP name	Meloxicam (mg)	PLGA* (mg)	Inorganic salt type	Inorganic salt (mg)	DCM (mL)
D	40	100	N/A	0	0.5
M4	40	100	$Mg(OH)_2$	4	0.5
M8	40	100	$Mg(OH)_2$	8	0.5
M12	40	100	$Mg(OH)_2$	12	0.5
P4	40	100	$Mg_3(PO_4)_2$	4	0.5
P8	40	100	$Mg_3(PO_4)_2$	8	0.5

* PLGA: Resomer 502 (7–17 kDa).

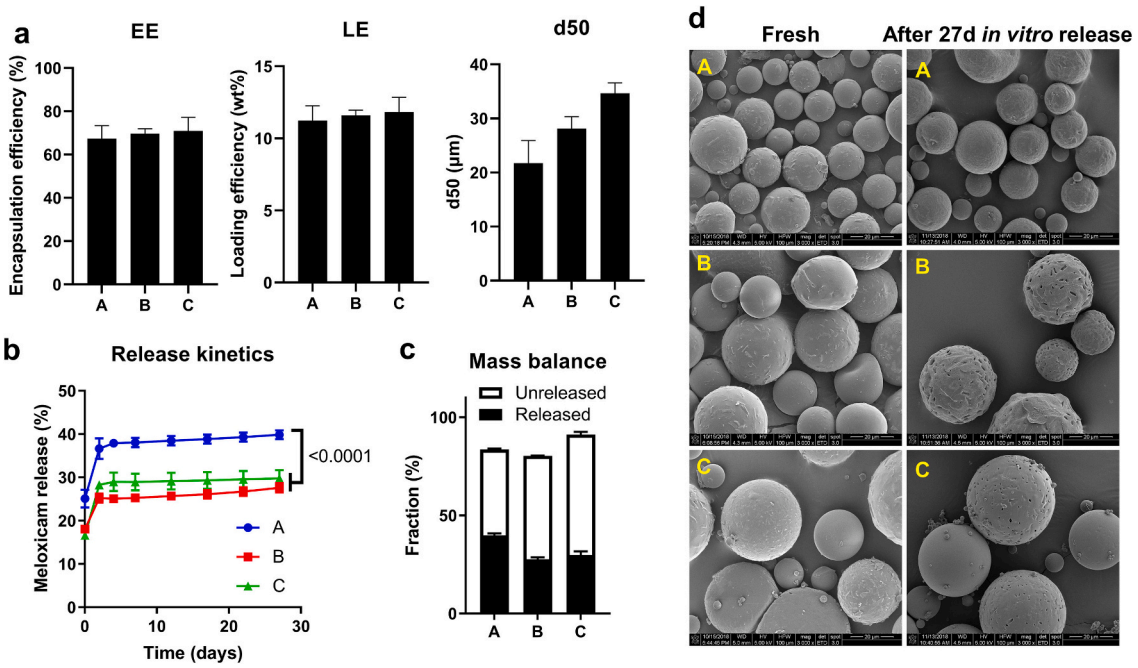

Fig. 1. Characterization of meloxicam-loaded PLGA MPs in Table 1. (a) Properties of meloxicam-loaded PLGA MPs. EE: encapsulation efficiency, LE: loading efficiency, d50: volume median diameter; (b) *In vitro* release kinetic profiles (*P* value: <0.0001, A *vs.* B or C on day 27 by Tukey's multiple comparison's test) and (c) mass balance of meloxicam from meloxicam-loaded PLGA MPs; (d) SEM images of meloxicam-loaded PLGA MPs, fresh (left) and after 27-day *in vitro* release study (right).

Table 3
Microparticle (MP) optimization by DoE response surface model.

Variables				Responses					
X_1, α-value of $Mg(OH)_2$	X_2, α-value of meloxicam	$Mg(OH)_2$ (mg)	Meloxicam (mg)	EE* (%)	LE* (%)	d50* (μm)	Cumulative release in 8 h (Burst release) (%)	Cumulative release in 7d (%)	Drug release slope k (8 h-7d)
0	0	8	40	84.4	22.8	42.3	30.4	53.1	11.8
−1	−1	4	20	81.2	13.1	36.0	29.5	46.9	9.6
1	−1	12	20	59.4	9.0	35.7	32.4	72.6	21.3
1	1	12	60	75.4	26.3	46.0	44.9	62.8	9.6
−1	1	4	60	76.5	28.0	43.4	29.1	44.2	6.7
0	0	8	40	74.0	20.0	46.3	25.2	56.2	16.6
0	0	8	40	74.0	20.0	41.3	27.7	57.7	15.9
−1.414	0	2.3	40	77.2	21.7	43.5	26.9	37.0	5.2
0	0	8	40	73.3	19.8	45.2	27.8	52.5	13.2
0	1.414	8	68.3	74.1	28.7	50.0	62.5	79.3	8.8
0	0	8	40	75.1	20.3	45.0	26.9	54.0	14.3
1.414	0	13.7	40	48.8	12.7	41.6	71.8	103.8	17.2
0	0	8	40	78.1	21.1	45.7	31.4	52.9	11.4
0	−1.414	8	11.7	56.3	5.5	36.7	26.5	58.2	16.2
0	0	8	40	78.8	21.3	42.4	30.3	58.6	14.9
0	0	8	40	74.7	20.2	36.8	29.3	54.9	13.4

* EE: encapsulation efficiency; LE: loading efficiency; d_{50}: volume median diameter.

Table 4
Formulation of PLGA MPs with predicted release kinetics.

MP name	Burst release (8 h)[a]	Later-stage release (8 h–7 day)[b]	$Mg(OH)_2$ (mg)	Meloxicam (mg)	Meloxicam loading (%)	$Mg(OH)_2$ loading (%)	Burst release (8 h)		Later-stage release slope (8 h–7 day)	
							Prediction (%)	Experimental data (%)[c]	Prediction	Experimental data[d]
E1	Low	Low	4	40	25.3	3.01	27.8	23.0 ± 0.8	8.24	6.76 ± 0.37
E2	Low	Medium	7	30	19.6	5.38	24.9	23.4 ± 2.3	13.8	14.8 ± 0.94
E3	Medium	Medium	11	50	25.5	6.93	46.6	35.3 ± 2.3	13.4	15.4 ± 1.2

[a] Burst release (8 h): <34%, Low; > 61%, High; 34–61%, Medium.
[b] Later-stage release slope: <9.4, Low; >18.1, High; 9.4–18.1, Medium.
[c] $n = 3$ tests of a single batch; mean ± standard deviation.
[d] Generated with the average cumulative release ($n = 3$); slope (best fit) ± standard error

where Y is the response variable (such as initial burst release or drug release slope); X_1 and X_2 are independent variables (α-values of $Mg(OH)_2$ and meloxicam); b_0 is the intercept coefficient; b_1 and b_2 are coefficients of linear terms (X_1, X_2); b_{12} is a coefficient of the interaction term (X_1X_2); b_{11} and b_{22} are coefficients of quadratic terms (X_1^2 and X_2^2). Quadratic terms are included to model the curvature across the response surface.

All the particles were prepared by the S/O/W method as described in Section 2.2.2, with 2.3–13.7 mg $Mg(OH)_2$ and 11.7–68.3 mg meloxicam (Table 3), 100 mg PLGA (L:G = 50:50; ester-end; 7–17 kDa), and 0.5 mL of DCM.

2.2.4. Production of selected meloxicam-loaded MPs (E1-E3; Table 4)

According to the DoE analysis and prediction based on the JMP software (SAS Institute, Cary, NC, USA), three types of $Mg(OH)_2$-containing MPs were formulated to generate three different release kinetics profiles. All the particles were prepared by the S/O/W method with 100 mg PLGA (L:G = 50:50; ester-end; 7–17 kDa) and 0.5 mL of DCM as described in Section 2.2.2.

2.3. Microparticle (MP) characterization

The size of meloxicam-loaded PLGA MPs was measured by a CILAS 1190 laser diffraction particle size analyzer (Orleans, France). For microscopic observation, the MPs were pre-coated with platinum using a Cressington turbo-pumped sputter coater (Cressington Scientific Instrument, Watford, UK) and imaged with an FEI NOVA nanoSEM scanning electron microscope (SEM). To determine the meloxicam loading content, 2 mg of meloxicam-loaded MPs was weighed and dissolved in 1 mL of DMSO. To the MP solution, 1 mL of DI water was added to precipitate PLGA. With a target loading of <30 wt%, this solution should contain no >300 μg/mL of meloxicam, which is lower than the solubility of meloxicam in 50% DMSO (398.8 μg/mL). Therefore, meloxicam is expected to be fully recovered in supernatant. PLGA precipitate was separated by centrifugation at 12,126 RCF for 5 min, and the supernatant containing meloxicam was analyzed by high-pressure liquid chromatography (HPLC). The drug loading content was defined as the amount of encapsulated meloxicam divided by the weight of MPs.

2.4. In vitro meloxicam release kinetics

Meloxicam-loaded MPs were dispersed in 1.8 mL of phosphate buffered saline containing 0.05 *w/v*% Tween 80 (PBST) at a concentration equivalent to 100 μg/mL meloxicam. The MP suspension was put in 2-mL capacity Eppendorf tube and rotated at 10 rpm on a tube revolver rotator (Thermo Scientific) at 37 °C. At each time point, the MP suspension was centrifuged at 5000 RCF for 5 min, and 1.6 mL of supernatant was sampled for HPLC analysis and replaced with the same volume of fresh release medium. After the last sampling, the MP pellets were analyzed by the same technique as fresh MPs to quantify residual meloxicam in the MPs. The solubility of meloxicam in PBST at 37 °C was measured to be 297 μg/mL. Unless all the loaded meloxicam is released at once, the concentration of released meloxicam would be kept far below the solubility limit by frequent exchange of release medium (89% replacement with fresh PBST at each time point); thus, the MP concentration was deemed to satisfy sink condition (≤ 1/3 of saturation solubility [20–23]).

In the specified studies, the release kinetics were performed with dialysis bags. The molecular weight cut-offs (MWCOs) of dialysis bags were varied to generate differential delays in transferring the released drug to the release medium (sink). Specifically, the MPs (E1 and E3) equivalent to 0.8 mg of meloxicam were suspended in 1 mL of PBST contained in a dialysis bag with a MWCO of 0.5–1 kDa, 3.5–5 kDa, or 20 kDa. These were dialyzed against 10 mL of PBST at 37 °C under constant agitation. At selected time points, 1 mL of the release medium was collected and replaced with 1 mL of fresh PBST. Meloxicam content in the sampled release medium was measured by HPLC.

2.5. High-pressure liquid chromatography (HPLC) analysis of meloxicam

Meloxicam was quantified by an Agilent 1290 HPLC system (Santa Clara, CA, USA) equipped with a C18 Phenomenex Luna column (100 Å, 250 × 4.6 mm). The mobile phase was a mixture of acetonitrile and 50 mM pH 6.5 phosphate buffer (30:70, *v/v*) and flowed at 0.8 mL/min for 20 min. Meloxicam was detected at 355 nm with a retention time of 10.8 min.

2.6. Pharmacokinetics of subcutaneously injected meloxicam-loaded MPs

Male Sprague Dawley rats were obtained from Envigo (Indianapolis, IN, USA) at 330–365 g (average 353 g). All rats were individually housed in a temperature-controlled room under a 12 h light, 12 h dark cycle and fed standard pelleted chow (2014 Teklad, Envigo). Drinking water was available *ad libitum*. All animal procedures were approved by the Institutional Animal Care and Use Committee at Eli Lilly and Company. At the start of the study, rats were weighed and then anesthetized with isoflurane. The hair was clipped from the injection site.

For the treatment groups, the meloxicam-loaded MPs (E1, E2, and E3) equivalent to 1.9 mg meloxicam were suspended in 0.2 mL of sterile-filtered (0.2 μm pore size) diluent consisting of 0.5% sodium carboxymethyl cellulose, 0.1% Tween 80, and 0.9% NaCl in DI water. For the control group, a commercial solution containing 1 mg meloxicam (Alloxate 5 mg/mL, Patterson Veterinary, Lot: 820394A) was used. The rats were administered with one of the MPs or meloxicam solution by subcutaneous injection *via* 22G needle and syringe (n = 4 per group). Another group was administered a tail vein intravenous (IV) injection of a commercial solution containing 2 mg meloxicam (Alloxate 5 mg/mL, Patterson Veterinary, Lot: 810392D) to obtain the absolute bioavailability for the MP formulations.

Rats were returned to normal housing once conscious. Rats were serially bled *via* tail clip into ethylene diamine tetra-acetic acid (EDTA)-containing tubes at the following time points (1, 2, 4, 6, 12, 24, 48, 72, 96, 120, 144, 168, 192, 216, 240, 264, 288, 312, and 336 h post-injection) to obtain the meloxicam plasma concentrations. Plasma samples were submitted to Q2 Solutions (Indianapolis, IN) for analysis. After collecting the 336-h blood sample, the rats were euthanized with CO_2.

2.7. Pharmacokinetics (PK) analysis and the development of an in-vitro-in-vivo correlation (IVIVC)

Pharmacokinetics (PK) analysis was performed as we previously described [9] to obtain the PK parameters from the rat plasma concentration-time profiles following the subcutaneous injection of the meloxicam-loaded MP formulations. IVIVC analysis was performed using the Phoenix® IVIVC Toolkit (Certara USA, Inc., Princeton, USA). First, the *in vitro* release data were used as inputs and fitted to the Makoid-Banakar model. The plasma concentration and dosing data were mapped to the IVIVC object. Subsequently, a unit impulse response (UIR) function was determined from the mean concentration-time profile obtained with IV bolus administration. Deconvolution was performed to compute the fraction absorbed over time. Finally, an IVIVC relationship between the fraction of drug released *in vitro* ($F_{rel,\ in\ vitro}$) and the fraction of drug absorbed *in vivo* (F_{abs}) was fitted to the data for each MP formulation. The internal predictability of the model was also evaluated, where the IVIVC model was used to predict each formulation's plasma concentration profile from the *in vitro* release kinetics.

2.8. Statistical analysis

All statistical analyses were performed with GraphPad Prism 9 (La Jolla, CA, USA). All data were presented as mean ± standard deviation

(SD) of $n = 3$ replicates of a representative batch unless specified otherwise. Data were analyzed with a one-way or two-way ANOVA test to determine the statistical difference of means among various groups, followed by the recommended multiple comparisons tests. A value of $P < 0.05$ was considered statistically significant.

3. Results and discussion

3.1. Meloxicam encapsulation in PLGA MPs

Meloxicam-loaded PLGA MPs were initially produced by the O/W emulsion method varying the MW of PLGA (7–17 kDa, A; 24–38 kDa, B; and 38–54 kDa, C) (Table 1). PLGA and meloxicam were dissolved in a mixture of DCM and DMSO, where DMSO was used to help dissolve meloxicam. Meloxicam was encapsulated with an encapsulation efficiency (EE, loaded drug/feed drug) of 67.4%–71.0%, resulting in a loading efficiency (LE, drug/MP) of 11.2–11.8 wt%. The EE and LE showed no specific trend corresponding to the PLGA MW (**Fig. 1**a). The particle size increased with PLGA MW from 21.7 ± 4.2 μm (7–17 kDa, A) to 34.7 ± 1.9 μm (38–54 kDa, C), which may be attributed to the increasing viscosity of the organic phase. The MPs showed an initial burst release in 2 h, and no further release followed over the next 27 days. The extent of initial burst release was greater for the MPs made with a lower MW PLGA (A), but the MW of PLGA had no apparent influence on the later-phase drug release (**Fig. 1**b). The unreleased portion of meloxicam after 27-day incubation in PBST, ranging from 43.7 to 61.4% of the total loaded drug, was recovered from the remaining MPs (**Fig. 1**c). Of note, the total recovery (released + unreleased) is <100% in all three MPs, which likely reflects cumulative sample loss during the repeated sampling. Microscopic observation found no significant changes in MP morphology after the release kinetics study, except for slightly roughened surfaces (**Fig. 1**d), indicating that none of the MPs underwent apparent degradation in 27 days.

The initial burst release seen with A, B, and C MPs was attributed to the increased molecular mobility of the drug and polymer chains in the hydrated MPs [7]. The relatively high burst release of A MPs may be explained by the small MW of PLGA (7–17 kDa) compared to that of B and C MPs (24–54 kDa), which would facilitate chain movement. The lack of later-phase release may also be explained by the increased mobility of polymer chains, which leads to reconfiguration of the MP skin layer into a dense diffusion barrier [7]. Moreover, given the pH-dependent solubility of meloxicam [17], we may not rule out the possibility of meloxicam becoming increasingly insoluble in the developing acidity of MP matrices due to PLGA degradation.

3.2. Control of drug release kinetics

To suppress the initial burst release and enhance the later phase drug release, we made two modifications to 7–17 kDa PLGA MPs: addition of meloxicam as solid particles and inclusion of $Mg(OH)_2$ as a drug release modifier (Table 2). First, meloxicam was suspended in the organic phase as solid particles by omitting DMSO (solvent for meloxicam). We expected that the solid form of poorly soluble meloxicam would dissolve slowly with time and reduce the initial burst release. Additionally, the dissolved meloxicam may leave fluid channels behind to overcome the densifying surface layer and facilitate later-phase drug release [9]. Encapsulating meloxicam as a solid also helped increase the meloxicam/PLGA loading ratio. Second, $Mg(OH)_2$ was added to maintain the solubility of meloxicam by neutralizing the acidifying microenvironment of PLGA MPs in the later phase [19]. The literature suggests the presence of residual monomers (lactic acid and glycolic acid) in commercial PLGA [24]; therefore, we expected that $Mg(OH)_2$ may impact drug release even before PLGA started to degrade.

According to HPLC chromatograms of meloxicam before and after microencapsulation, meloxicam remained stable during encapsulation with $Mg(OH)_2$. Meloxicam was also stable in PBST at 37 °C in the presence of maximum possible $Mg(OH)_2$ at least for 17 days (duration of observation; Supporting Fig. 2), ruling out detrimental effects of $Mg(OH)_2$ on meloxicam during the release testing. As evident from the comparison with A MPs (Fig. 1), D MPs produced by the S/O/W emulsion method (*i.e.*, encapsulating meloxicam as solid particles) showed much lower initial burst release than A MPs (produced by the O/W emulsion method), but the later-phase drug release continued to be limited (Fig. 2). However, with the addition of $Mg(OH)_2$ (M MPs), meloxicam release continued for 7 days (**Fig. 2**a, left), reaching 77.6% drug release in 7 days with the highest $Mg(OH)_2$ content tested (M12). Another noticeable difference between M MPs and A MPs was a dramatic change of the morphology in 14 days, from solid fresh MPs to mostly shattered fragments (**Fig. 2**b,c; Supporting Fig. 3), which suggests that the solid form of meloxicam and/or $Mg(OH)_2$ may have accelerated the disintegration of MPs by generating fluid channels. On the other hand, an alternative salt, *i.e.*, $Mg_3(PO_4)_2$, with comparable solubility [water solubility estimated from solubility product constants (K_{sp}) [25]: 6.5 μg/mL for $Mg(OH)_2$ and 4.9 μg/mL for $Mg_3(PO_4)_2$] but low basicity, did not affect later-phase drug release (P4, P8) (**Fig. 2**a, right). The morphology of P8 MPs also did not change as dramatically as M8 MPs in 14 days of release test (Supporting Fig. 3c). These differences suggest that the main contribution of $Mg(OH)_2$ to the meloxicam release is to neutralize the MP matrices, thereby maintaining the solubility of meloxicam, rather than to form fluid channels. Meanwhile, given the relatively large size of $Mg_3(PO_4)_2$ (20.9 ± 2.2 μm compared to 3.4 ± 0.14 μm of $Mg(OH)_2$) (Supporting Fig. 1), the ineffectiveness of $Mg_3(PO_4)_2$ may be attributable not only to the lack of basicity but also to the relatively inefficient encapsulation of the salt, *i.e.,* a lower salt content.

3.3. Design of Experiments (DoE) for release kinetics control from Mg(OH)$_2$-containing MPs

To compare the impact of each formulation component on the release kinetics control, we used DoE with a central composite design to generate the response surface and produced $Mg(OH)_2$-containing MPs accordingly, varying the levels of $Mg(OH)_2$ content and meloxicam load (variables). Two responses (the extent of *in vitro* drug release by the first 8 h and the later-phase [8 h – 7 days] drug release rate, *k*) were fitted to the response surface model as a function of the two variables (**Fig. 3**a)

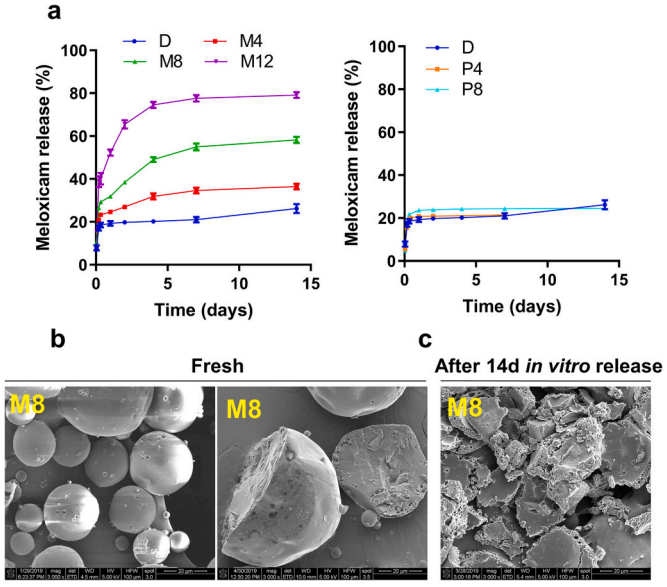

Fig. 2. (a) *In vitro* meloxicam release kinetic profiles from modified meloxicam-loaded PLGA MPs (Table 2); (b) SEM images of fresh M8 MPs (left: intact; right: cryo-fractured to reveal the cross-section); (c) SEM image of M8 MPs after 14-day *in vitro* release study (right).

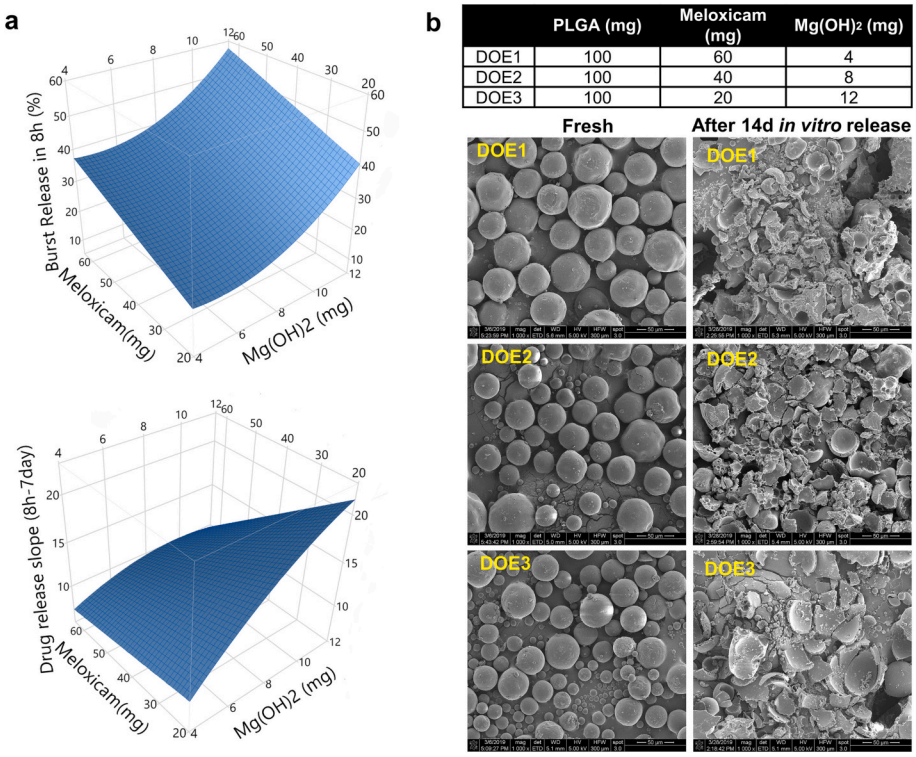

Fig. 3. (a) 3D surface plot to identify the effects of critical process parameters on release kinetics; (b) SEM images of three MPs from DoE (Table 3), fresh (left) and after 14-day *in vitro* release study (right).

via the following equations for the modeling.

$$Y_1(\text{first 8h drug release}) = 30.975 + 10.275X_1 + 7.877X_2 + 7.126{X_1}^2$$
$$Y_2(\text{later drug release slope k}) = 13.5720 + 3.9466X_1 - 3.1334X_2 - 2.2X_1X_2 - 1.3816{X_1}^2$$
$$X_1 = \text{Mg(OH)}_2\ \alpha\ \text{value};\ X_2 = \text{Meloxicam}\ \alpha\ \text{value}$$

Increasing meloxicam load increased the initial release by 8 h but reduced the later-phase drug release. Increasing $Mg(OH)_2$ increased both the initial and later-phase drug release. These trends suggest that the sustained dissolution of solid drug and $Mg(OH)_2$ primarily influenced the drug release in the early phase, whereas the later phase depended on the balance of the amount of undissolved meloxicam and the availability of $Mg(OH)_2$ to help dissolve meloxicam. Selected MPs in this series showed significant changes in morphology under SEM after 14-day *in vitro* release studies (Fig. 3b), consistent with the pilot study (Supporting Fig. 3), supporting the contribution of solid meloxicam and $Mg(OH)_2$ to the creation of fluid channels and disintegration of MPs.

3.4. *In vivo pharmacokinetics and deconvolution of in vivo release profiles of selected MPs*

Based on DoE analysis, we produced three $Mg(OH)_2$-including formulations with different levels of initial and later-phase drug release (Table 4, **Fig. 4**a). The *in vitro* release kinetics of the three MPs were close to those estimated by the response surface model, *i.e.*, E3 (highest meloxicam and $Mg(OH)_2$ loading) showed the highest burst release (Table 4), and E1 and E2 showed differential later-phase release corresponding to the $Mg(OH)_2$ content relative to the meloxicam load. The morphology change after 14-day *in vitro* release studies (Supporting Fig. 4) was also similar to those tested in DoE (**Fig. 3**b). Of note, despite the enhanced later-phase release compared to D MP (**Fig. 2**a), all three MPs showed a plateau in release kinetics after 7 days (**Fig. 4**a). We suspect that $Mg(OH)_2$ may have been insufficient relative to the content of meloxicam solid for enhancing its dissolution. The optimal ratio of $Mg(OH)_2$ to meloxicam for complete release remains to be identified in future studies.

The three MPs were subcutaneously injected into rats for PK analysis to evaluate whether the *in vitro* release translates to *in vivo* release. The plasma concentration profiles of the three MPs are shown in **Fig. 4**b. Non-compartmental analysis was performed, and the key PK parameters are listed in Table 5. The subcutaneous bolus injection of meloxicam solution induced a relatively rapid absorption of meloxicam with a T_{max} of 4.5 h and C_{max} of 64,000 nM. All three MPs showed a delayed absorption of meloxicam with a T_{max} of 10.5–15 h and a C_{max} of 9780–15,400 nM and kept meloxicam plasma levels higher than those of subcutaneous bolus injection after the initial absorption period, indicating that the drug continued to be release over 14 days. Out of the three MPs, the E2 formulation had the highest absolute bioavailability, followed by E1 and E3.

3.5. *In vitro-in vivo correlation (IVIVC)*

Fig. 4c shows the estimated *in vivo* drug release profiles overlaid on the *in vitro* release for E1, E2, and E3 MPs. The *in vivo* curves show biphasic release profiles consisting of an initial burst release followed by a secondary release, consistent with *in vitro* release. While the *in vivo*

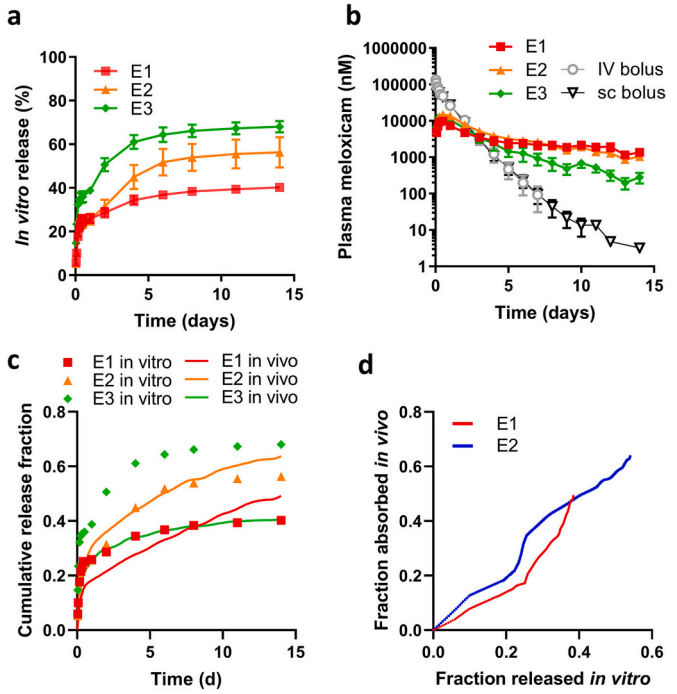

Fig. 4. (a) *In vitro* release kinetics of meloxicam from selected meloxicam-loaded MPs (Table 4). (b) Mean plasma concentration-time profiles of meloxicam in rats following IV [9] and subcutaneous (SC) administration of a meloxicam bolus solution and SC injection of E1, E2, and E3 MPs ($n = 4$ per group). IV dose: 2 mg meloxicam, SC dose: 1 mg meloxicam, MP dose: equivalent to 1.9 mg meloxicam; (c) Estimated *in vivo* release profiles overlaid on *in vitro* release of meloxicam after SC injection of MPs; (d) IVIVC developed with E1 and E2.

profiles for the E1 and E2 MPs follow the same trends as the *in vitro* release profiles, the *in vivo* data for the E3 MP deviates from the trend. In addition, the *in vitro* and *in vivo* drug release data for E1 and E2 do not accurately fit the full *in vivo* profiles. The validity and internal predictability of an IVIVC were initially assessed with all three MPs; as expected, the model was not predictive based on the calculated average percent prediction errors (% PE) for AUC and C_{max}, which were ~ 30% and ~ 20%, respectively.

Since a minimum of two datasets is required to build an IVIVC, we attempted to establish a point-to-point (level A) mathematical relationship between the observed *in vitro* and *in vivo* drug release rates using the E1 and E2 MPs (Fig. 4d). The predictability of the IVIVC was validated by comparing the simulated plasma concentration profiles from E1 and E2 with their respective observed plasma concentrations.

Table 5
Mean pharmacokinetic parameters in rats following subcutaneous administration.

Treatment group	AUC (nM*h) (CV%)	C_{max} (nM) (CV%)	T_{max} (h) (CV%)	Bioavailability (F, %)
E1	999,000 (34.7)	9780 (18.3)	12 (0)	54
E2	1,320,000 (14.9)	15,400 (13.4)	15 (40)	71
E3	848,000 (55.7)	14,000 (49.5)	10.5 (28.6)	46
Subcutaneous bolus	1,710,000 (3.4)	64,000 (6.85)	4.5 (42.5)	92

E1, E2, and E3 MPs: equivalent to 1.9 mg meloxicam; subcutaneous bolus: 1 mg meloxicam.
AUC: Area under the curve; C_{max}: Maximum plasma concentration; T_{max}: Time at which C_{max} is observed; CV: coefficient of variation.

The model predicted the plasma concentration profiles with an average % PE of AUC of ~10% but overestimated C_{max} for E1, resulting in a % PE of >20% (Supporting Table 1). No dataset was used for external validation.

Although E1 and E2 showed consistent trends between *in vitro* and *in vivo*, the internal validation did not meet the requirements stated in the FDA guidance to demonstrate predictive *in vivo* performance from *in vitro* release (% PE < 20%) [26], *i.e.*, the current *in vitro* release profiles may not adequately predict *in vivo* performance of the MPs. The large % PE may have resulted from the limitations of an *in vitro* release model, such as the difference in hydrodynamic conditions (constantly agitated *in vitro vs.* stagnant *in vivo*) and the overly simplified models of subcutaneous interstitial fluid [27] or matrices. These limitations are shared by many *in vitro* release methods. In a recent study, Bender et al. evaluated various *in vitro* tools to predict *in vivo* absorption post-SC administration and found that no particular *in vitro* tool could reliably predict *in vivo* bioavailability [28].

3.6. Explanation for deviation of E3 from level A IVIVC

The deviation of E3 from the level A IVIVC may be explained by the relatively high early-phase release. When a drug has a limited water solubility, the initial burst release may manifest differential effects between *in vivo* subcutaneous tissue and *in vitro* release study conditions, where the former has limited interstitial fluid and the latter is performed in release medium with a volume sufficient to satisfy the sink condition. To test this hypothesis, we repeated the *in vitro* release kinetics of E1 (slow release kinetics) and E3 (fast release kinetics) using dialysis bags with three different MWCOs (0.5–1 kDa, 3.5–5 kDa, and 20 kDa), which generate differential delay in drug diffusion across the membrane [29]. A delayed diffusion would induce precipitation of a poorly soluble drug inside the bag when the drug release is fast and the concentration exceeds the solubility limit [30,31] (Fig. 5a). Therefore, the release kinetics performed with a dialysis bag of a relatively low MWCO may simulate an aspect of the subcutaneous tissue, where the fast-released drug may precipitate before it is absorbed to the capillaries.

As expected, E3 showed highly variable release kinetics depending on the MWCO of the dialysis bag that housed the MP. E3 in the bag with

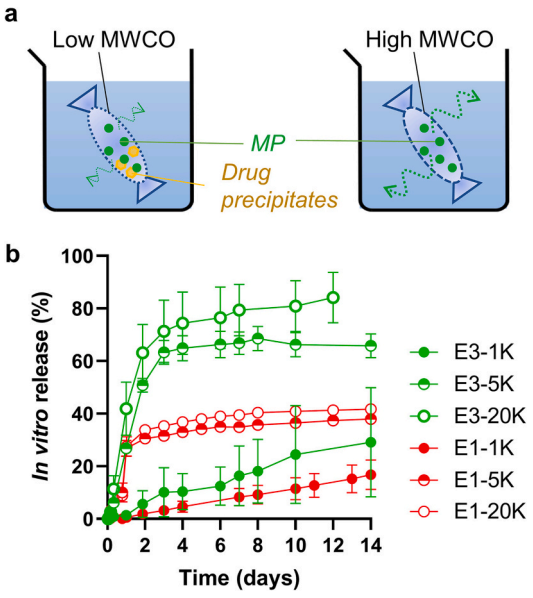

Fig. 5. (a) Schematic of alternative *in vitro* release kinetics study design; (b) *In vitro* release kinetics of meloxicam from E1 and E3 MPs in dialysis bags with different MWCOs (1 K: 0.5–1 kDa, 5 K: 3.5–5 kDa; 20 K: 20 kDa). $n = 3$ tests of a representative batch, mean ± SD. Error bars for E1-1K and E1-5K are small and hidden behind the symbols.

a MWCO of 0.5–1 kDa showed a slow and low-level drug release compared with those in higher MWCO bags (Fig. 5b). E1 showed a similar trend, but the extent of overall drug release was lower, and the difference was smaller than that of E3. This result suggests that the fast release of a poorly soluble drug may result in premature precipitation when its transfer to the sink (*i.e.*, the receiving medium *in vitro*; blood *in vivo*) is delayed by a low MWCO dialysis bag and in subcutaneous tissue, respectively. Therefore, the deviation of E3 MP from IVIVC may be attributable to the delayed absorption and subsequent precipitation of the initially released meloxicam. Given the high bioavailability (92%), we do not suspect that the precipitation would occur with bolus subcutaneous injection of meloxicam solution (Alloxate®), which is formulated with multiple components aiding in the solubilization of the drug (alcohol, glycofurol, poloxamer 188, and meglumine) [32]. However, meloxicam released from the E3 MP may be prone to precipitation without solubilizers to maintain the solubility.

4. Conclusions

We developed PLGA MPs that could deliver meloxicam over a period of 2 weeks. The initial burst release was controlled by encapsulating meloxicam in the solid state. The inclusion of $Mg(OH)_2$ helped enhance drug release in the later-phase phase by neutralizing the developing acidity of the PLGA MP microenvironment, which would otherwise limit the dissolution of meloxicam. The DoE demonstrated that the variation of solid meloxicam and $Mg(OH)_2$ contents enabled tunable control of meloxicam *in vitro* release profiles, resulting in three MP formulations with distinct release kinetics. Upon PK analysis in rats, two MPs with slower *in vitro* release kinetics showed a consistent trend in *in vivo* drug absorption as *in vitro* results. However, the MP with relatively high initial burst release deviated from *in vitro* prediction, which may be attributed to the precipitation of fast-released meloxicam prior to the absorption.

CRediT authorship contribution statement

Yihua Pei: Conceptualization, Methodology, Investigation, Writing – original draft, Writing – review & editing. **Jianping Wang:** Methodology, Investigation, Writing – original draft, Writing – review & editing. **Nisar Ul Khaliq:** Methodology, Investigation, Writing – review & editing. **Fanfei Meng:** Methodology, Investigation, Writing – review & editing. **Kaoutar A. Oucherif:** Formal analysis, Writing – original draft, Writing – review & editing. **Jie Xue:** Formal analysis, Visualization, Writing – review & editing. **Sarena D. Horava:** Conceptualization, Writing – review & editing. **Amy L. Cox:** Investigation, Writing – review & editing. **Coralie A. Richard:** Conceptualization, Writing – review & editing. **Monica R. Swinney:** Conceptualization, Writing – review & editing. **Kinam Park:** Conceptualization, Writing – review & editing, Funding acquisition. **Yoon Yeo:** Conceptualization, Writing – original draft, Writing – review & editing, Visualization, Supervision, Project administration, Funding acquisition.

Data availability

Data will be made available on request.

Acknowledgements

This study was supported by Eli Lilly and Company. The authors also appreciate the administrative support of Drs. Thomas R. Verhoeven and James H. Parshall. Reshma Bharadwaj from Eli Lilly Services India Pvt. Ltd. provided technical writing and editing support.

Appendix A. Supplementary data

Supplementary data to this article can be found online at https://doi.org/10.1016/j.jconrel.2022.12.019.

References

[1] N.U. Khaliq, D. Chobisa, C.A. Richard, M.R. Swinney, Y. Yeo, Engineering microenvironment of biodegradable polyester systems for drug stability and release control, Ther. Deliv. 12 (2021) 37–54, https://doi.org/10.4155/tde-2020-0113.
[2] H. Park, A. Otte, K. Park, Evolution of drug delivery systems: From 1950 to 2020 and beyond, J. Control. Release 342 (2022) 53–65, https://doi.org/10.1016/j.jconrel.2021.12.030.
[3] R. Chou, D.B. Gordon, O.A. de Leon-Casasola, J.M. Rosenberg, S. Bickler, T. Brennan, T. Carter, C.L. Cassidy, E.H. Chittenden, E. Degenhardt, S. Griffith, R. Manworren, B. McCarberg, R. Montgomery, J. Murphy, M.F. Perkal, S. Suresh, K. Sluka, S. Strassels, R. Thirlby, E. Viscusi, G.A. Walco, L. Warner, S.J. Weisman, C.L. Wu, Management of Postoperative Pain: a clinical practice guideline from the American pain society, the American Society of Regional Anesthesia and Pain Medicine, and the American Society of Anesthesiologists' committee on regional anesthesia, executive committee, and administrative council, J. Pain 17 (2016) 131–157, https://doi.org/10.1016/j.jpain.2015.12.008.
[4] S.A. Schug, Do NSAIDs really interfere with healing after surgery? J. Clin. Med. 10 (2021) https://doi.org/10.3390/jcm10112359.
[5] H. Zhao-Fleming, A. Hand, K. Zhang, R. Polak, A. Northcut, D. Jacob, S. Dissanaike, K.P. Rumbaugh, Effect of non-steroidal anti-inflammatory drugs on post-surgical complications against the backdrop of the opioid crisis, Burns Trauma 6 (2018) 25, https://doi.org/10.1186/s41038-018-0128-x.
[6] Y. Yeo, K. Park, Control of encapsulation efficiency and initial burst in polymeric microparticle systems, Arch. Pharm. Res. 27 (2004) 1–12, https://doi.org/10.1007/BF02980037.
[7] K. Park, A. Otte, F. Sharifi, J. Garner, S. Skidmore, H. Park, Y.K. Jhon, B. Qin, Y. Wang, Potential roles of the glass transition temperature of PLGA microparticles in drug release kinetics, Mol. Pharm. 18 (2021) 18–32, https://doi.org/10.1021/acs.molpharmaceut.0c01089.
[8] K. Park, A. Otte, F. Sharifi, J. Garner, S. Skidmore, H. Park, Y.K. Jhon, B. Qin, Y. Wang, Formulation composition, manufacturing process, and characterization of poly(lactide-co-glycolide) microparticles, J. Control. Release 329 (2021) 1150–1161, https://doi.org/10.1016/j.jconrel.2020.10.044.
[9] Y.C. Chen, D.E. Moseson, C.A. Richard, M.R. Swinney, S.D. Horava, K.A. Oucherif, A.L. Cox, E.D. Hawkins, Y. Li, D.F. DeNeve, J. Lomeo, A. Zhu, L.T. Lyle, E. J. Munson, L.S. Taylor, K. Park, Y. Yeo, Development of hot-melt extruded drug/polymer matrices for sustained delivery of meloxicam, J. Control. Release 342 (2022) 189–200, https://doi.org/10.1016/j.jconrel.2021.12.038.
[10] W. Jiang, S.P. Schwendeman, Stabilization and controlled release of bovine serum albumin encapsulated in poly(D, L-lactide) and poly(ethylene glycol) microsphere blends, Pharm. Res. 18 (2001) 878–885, https://doi.org/10.1023/a:1011009117586.
[11] M. van de Weert, W.E. Hennink, W. Jiskoot, Protein instability in PLGA microparticles, Pharm. Res. 17 (2000) 1159–1167, https://doi.org/10.1023/a:1026498209874.
[12] C. Zlomke, M. Barth, K. Mader, Polymer degradation induced drug precipitation in PLGA implants - why less is sometimes more, Eur. J. Pharm. Biopharm. 139 (2019) 142–152, https://doi.org/10.1016/j.ejpb.2019.03.016.
[13] Meloxicam. https://go.drugbank.com/drugs/DB00814.
[14] D. Türck, W. Roth, U. Busch, A review of the clinical pharmacokinetics of meloxicam, Br. J. Rheumatol. 35 (Suppl. 1) (1996) 13–16, https://doi.org/10.1093/rheumatology/35.suppl_1.13.
[15] G. Engelhardt, D. Homma, K. Schlegel, R. Utzmann, C. Schnitzler, Anti-inflammatory, analgesic, antipyretic and related properties of meloxicam, a new non-steroidal anti-inflammatory agent with favourable gastrointestinal tolerance, Inflamm. Res. 44 (1995) 423–433, https://doi.org/10.1007/BF01757699.
[16] A. Bekker, C. Kloepping, S. Collingwood, Meloxicam in the management of post-operative pain: narrative review, J. Anaesthesiol. Clin. Pharmacol. 34 (2018) 450–457, https://doi.org/10.4103/joacp.JOACP_133_18.
[17] P. Luger, K. Daneck, W. Engel, G. Trummlitz, K. Wagner, Structure and physicochemical properties of meloxicam, a new NSAID, Eur. J. Pharm. Sci. 4 (1996) 175–187, https://doi.org/10.1016/0928-0987(95)00046-1.
[18] K. Fu, D.W. Pack, A.M. Klibanov, R. Langer, Visual evidence of acidic environment within degrading poly(lactic-co-glycolic acid) (PLGA) microspheres, Pharm. Res. 17 (2000) 100–106, https://doi.org/10.1023/a:1007582911958.
[19] A. Shenderova, T.G. Burke, S.P. Schwendeman, The acidic microclimate in poly (lactide-co-glycolide) microspheres stabilizes camptothecins, Pharm. Res. 16 (1999) 241–248, https://doi.org/10.1023/a:1018876308346.
[20] D.J. Phillips, S.R. Pygall, V.B. Cooper, J.C. Mann, Overcoming sink limitations in dissolution testing: a review of traditional methods and the potential utility of biphasic systems, J. Pharm. Pharmacol. 64 (2012) 1549–1559, https://doi.org/10.1111/j.2042-7158.2012.01523.x.
[21] B. Vaghela, R. Kayastha, N. Bhatt, N. Pathak, D. Rathod, Development and validation of dissolution procedures, J. Appl. Pharmaceut. Sci. 1 (2011) 50–56.
[22] U. Pharmacopeia, USP-NF<1092> the Dissolution Procedure: Development and Validation, USP 32-NF27, 2009.
[23] U. Pharmacopeia, USP-NF<1225> Validation of Compendial Methods, USP 32-NF27, 2009.
[24] M. Kohno, J.V. Andhariya, B. Wan, Q. Bao, S. Rothstein, M. Hezel, Y. Wang, D. J. Burgess, The effect of PLGA molecular weight differences on risperidone release from microspheres, Int. J. Pharm. 582 (2020), 119339, https://doi.org/10.1016/j.ijpharm.2020.119339.

[25] CRC Handbook of Chemistry and Physics, 102nd edition.CRC Press, Boca Raton, 2021.
[26] Guidance for Industry, Extended Release Oral Dosage Forms: Development, Evaluation, and Application of In Vitro/In Vivo Correlations, F.a.D.A. US Department of Health and Human Services, Rockville, MD, 1997.
[27] I. Torres-Terán, M. Venczel, S. Klein, Prediction of subcutaneous drug absorption - do we have reliable data to design a simulated interstitial fluid? Int. J. Pharm. 610 (2021), 121257 https://doi.org/10.1016/j.ijpharm.2021.121257.
[28] C. Bender, S. Eichling, L. Franzen, V. Herzog, L.M. Ickenstein, D. Jere, L. Nonis, G. Schwach, P. Stoll, M. Venczel, S. Zenk, Evaluation of in vitro tools to predict the in vivo absorption of biopharmaceuticals following subcutaneous administration, J. Pharm. Sci. (2022), https://doi.org/10.1016/j.xphs.2022.04.005.
[29] M. Yu, W. Yuan, D. Li, A. Schwendeman, S.P. Schwendeman, Predicting drug release kinetics from nanocarriers inside dialysis bags, J. Control. Release 315 (2019) 23–30, https://doi.org/10.1016/j.jconrel.2019.09.016.
[30] S.A. Abouelmagd, B. Sun, A.C. Chang, Y.J. Ku, Y. Yeo, Release kinetics study of poorly water-soluble drugs from nanoparticles: are we doing it right? Mol. Pharm. 12 (2015) 997–1003, https://doi.org/10.1021/mp500817h.
[31] S. Modi, B.D. Anderson, Determination of drug release kinetics from nanoparticles: overcoming pitfalls of the dynamic Dialysis method, Mol. Pharm. 10 (2013) 3076–3089, https://doi.org/10.1021/mp400154a.
[32] Alloxate: Product Information. https://vetlabel.com/lib/vet/meds/alloxate-2/.